Differential Code Bias Estimation using Multi-GNSS Observations and Global Ionosphere Maps

O. Montenbruck, A. Hauschild, *Deutsches Zentrum für Luft- und Raumfahrt (DLR/GSOC)*
P. Steigenberger, *Technische Universität München (TUM/IAPG)*

BIOGRAPHIES

Oliver Montenbruck is head of the GNSS Technology and Navigation Group at DLR's German Space Operations Center, Oberpfaffenhofen. His current research activities comprise spaceborne GNSS receiver technology, autonomous navigation systems, spacecraft formation flying and precise orbit determination as well as new constellations and multi-GNSS processing. Oliver Montenbruck presently chairs the GNSS Working Group of the International GPS Service and coordinates the performance of the MGEX Multi-GNSS Experiment. He authored numerous technical papers and various textbooks related to his fields of work.

André Hauschild is a member of the scientific staff of the GNSS Technology and Navigation Group at DLR's German Space Operations Center (GSOC). His field of work focuses on real-time precise orbit and clock estimation for GNSS satellites as well as multi-GNSS processing using modernized GPS and new satellite navigation systems. André graduated in aerospace engineering from Technische Universität Braunschweig, Germany, in March 2007 and received his Ph.D. from Technische Universität München, Germany, in July 2010.

Peter Steigenberger works at the Institute of Astronomical and Physical Geodesy of Technische Universität München (TUM, Munich, Germany). His current research interests include global GNSS solutions and the analysis of the GNSS-derived parameter time series, e.g., troposphere zenith delays, station coordinates, satellite orbits, and Earth rotation parameters.

ABSTRACT

Measurements of Global Navigation Satellite System (GNSS) receivers are affected by systematic offsets related to group and phase delays of the signal generation and processing chain. The resulting code and phase biases depend on the transmission frequency and the employed signal modulation. Within this study differential code biases (DCBs) of legacy and modernized GNSS signals are derived from pseudodrange observations of a global multi-GNSS receiver network. Global ionosphere maps (GIMs) are employed for the correction of ionospheric path delays. Satellite and receiver-specific contributions are separated based on the assumption of additive biases and a zero-mean condition for the satellite biases within a constellation. Based on 6 months of data collected within the Multi-GNSS Experiment (MGEX) of the International GNSS Service (IGS), DCBs for the publicly available signals of GPS, Galileo and BeiDou have been determined. The quality of the resulting DCB estimates is assessed and compared against group delay parameters transmitted by the GNSS providers as part of the broadcast ephemeris data.

INTRODUCTION

Pseudorange observations are well known to be affected by signal- and frequency-dependent differential code biases (DCBs) that need to be considered in the observation modeling. Depending on the choice of a conventional signal or signal combination for the clock offset determination, timing group delays (TGDs) or inter-signal corrections (ISCs) need to be applied when using other signals for pseudorange-based positioning.

DCBs and TGDs are routinely determined for the legacy GPS and GLONASS signals (C/A and P/Y code on L1 and L2) but only limited knowledge is presently available for satellite and receiver DCBs related to modernized GPS signals (L2C, L5) as well as those of new and emerging constellations (BeiDou, Galileo, QZSS, IRNSS).

Within the Multi-GNSS Experiment (MGEX) of the International GNSS Service (IGS) multi-frequency observations and broadcast navigation messages of the BeiDou and Galileo constellations as well as the QZS-1 satellite are collected on a routine basis by a global network of monitoring stations. These offer a basis for an independent determination of differential code biases for a wide range of signal combinations within a combined estimation of DCBs and ionospheric parameters.

As a simplified alternative, a multi-GNSS DCB estimation system has been established, which makes use of global ionosphere maps (GIMs) to model the contribution of ionospheric path delays on the difference of dual-frequency pseudoranges. DCBs of individual satellite-receiver combinations can thus be derived from an aver-

age of ionosphere-corrected pseudoranges differences over a given tracking arc for any combination of commonly tracked signals. Using a distributed network of monitoring stations and observations of all satellites within a constellation, the satellite-receiver DCBs may subsequently be partitioned into satellite-specific and receiver-specific DCBs. In accord with the common convention applied for GPS and GLONASS within the IGS, a zero-mean condition is applied for the constellation average of the satellite biases in this process.

Following a brief overview of the MGEX tracking network and the employed receiver types, the concept of DCB estimation with a priori ionosphere information is presented. Thereafter, results for legacy and modernized GPS signals as well as Galileo and BeiDou are presented and discussed. To assess the achievable accuracy, DCBs for legacy GPS signals are compared against DCBs derived routinely by the Center for Orbit Determination in Europe (CODE) from the much larger core IGS network. Furthermore, DCBs for new constellations are compared against broadcast group delay parameters determined by the GNSS providers.

TRACKING NETWORK AND RECEIVERS

In response to the ongoing modernization of legacy GNSSs (GPS, GLONASS) and the rapid build-up of multiple new satellite navigation systems (BeiDou, Galileo, QZSS, IRNSS), the International GNSS Service (IGS) has established the Multi-GNSS Experiment (MGEX; [1]) as a platform for early familiarization with new systems and signals. Starting in early 2012 a new network of multi-GNSS receivers was established in parallel to established GPS/GLONASS stations. By the end of 2013, the MGEX network has already grown to roughly 90 stations (Figure 1) and offered a global coverage for Galileo and BeiDou satellites in medium-altitude Earth orbits (MEOs) as well as regional coverage of the QZSS and BeiDou satellites in inclined geosychronous and geostationary orbits (IGSs/GEOs).

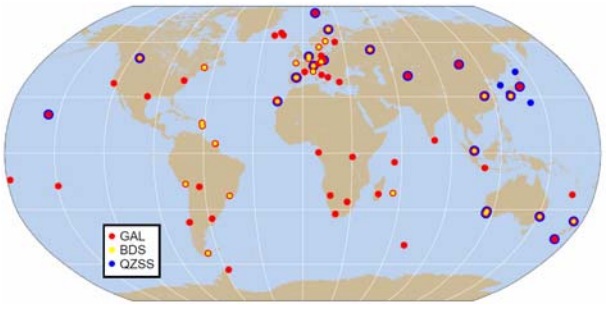

Figure 1 MGEX station distribution and supported constellations (Dec. 2013)

Other than various private multi-GNSS networks deployed by companies such as Trimble or Fugro, the MGEX network is highly heterogenous. It makes use of a wide variety of receivers and antennas as well as diverse combinations thereof. An up-to-date overview of the MGEX network and the employed hardware is available through the MGEX website [2].

For the period covered by this study (Jan.-June 2013), the MGEX network had not reached its current deployment status and was therefore augmented by stations of the COperative Network for GNSS Observations (CONGO) that joined the MGEX network at a later stage. A summary of contributing receivers and their observation types is provided in Table 1. Overall, GPS, Galileo, and BeiDou observations from up to 85 receivers were incorporated into the DCB analysis. While the majority of these receivers also tracks the (legacy) GLONASS signals (C/A- and P-code on L1 and L2), the estimation of GLONASS DCBs is already well covered by the IGS and beyond the scope of the present study. Likewise, QZSS has been excluded from the analysis, since the availability of only a single spacecraft does not enable a proper separation of satellite and receiver DCBs without a calibrated reference station.

Table 1 Receiver and observation types used for the estimation of differential code biases. Observation types for GPS (G) Galileo (E), BeiDou (C) are based on RINEX 3 observation codes [3].

Receiver Type	Sites	Observations
Javad TR_G2T, TRE_G3TH	29	G: 1C,1W,2X,2W,5X E: 1X,5X
Javad TRE_G3TH (v8 board)	1	G: 1C,1W,2X,2W,5X E: 1X,5X,7X,8X C: 2I,7I
Trimble NETR9	29	G:1C,2X,2W,5X E: 1X,5X,7X,8X C: 2I,6I,7I
Leica GR10, GR25, GRX1200+GNSS	14	G: 1C,2S,2W,5Q E: 1C,5C,7C,8Q
NovAtel OEM6	1	G: 1C,2W,5Q E: 1C,5Q
Septentrio AsteRx3, PolaRxS/4/4TR	11	G: 1C,2L,2W,5Q E: 1C,5Q,7Q,8Q C: 2I,7I

Most modernized GNSS signals offer distinct data-less (pilot) signal components in parallel to those modulated with navigation data. These pilot signals are considered to facilitate a robust signal tracking under adverse conditions, since the coherent integration time is not limited by bit transitions. Inspection of Table 1 shows that the currently available multi-GNSS receivers can largely be divided into two categories with respect to tracking of such signals. While part of the receivers (Septentrio, NovAtel, Leica) provide pilot-only observations, others (Javad, Trimble) provide measurements from a combined pilot+data tracking. In case of the GPS L2C signal, a total of three flavors can even be encountered: observations derived from tracking of the medium length L2C(M) code with navigation data (Leica), the long L2C(L) pilot component (Septentrio) or the combined L2C(L+M) signal (Javad, Trimble).

Other than specialized Test User Receivers [4] which may support concurrent (or at least configurable) tracking and measurement generation for multiple signal components, only a single, predefined tracking mode is usually available in commercial multi-GNSS receivers. For the determination of differential code biases it is, nevertheless, important to carefully distinguish different tracking modes, since the satellite contribution to the observed receiver-plus-satellite DCB may depend on the particular signal component(s) selected for the tracking. In accord with this consideration, distinct group delay corrections will be broadcast for the I- and Q-components of the GPS (and QZSS) L5 and L1C signals ([5]-[6]). For L2C, only a single Inter-Signal Correction (ISC) parameter is presently available as part of the CNAV navigation message [7]. However, no public evidence has been provided so far, that the biases between the L2C signal components are indeed small enough to be neglected in practice. For precision applications in geodesy and surveying, distinct DCBs for the various L2C components should therefore be derived from actual observations.

DCB ESTIMATION

The estimation of differential code biases has long been established as an integral part of ionospheric monitoring from terrestrial and spaceborne GPS/GLONASS observations (see [8]-[10] and references therein). DCBs are routinely estimated by IGS Analysis Centers and reported as part of Global Ionosphere Maps (GIMs) in Ionosphere map Exchange format (IONEX, [11]) or as independent DCB products.

Ignoring multipath and noise, a single pseudorange observation

$$P = \rho + c\delta t^{\mathrm{rcv}} - c\delta t^{\mathrm{sat}} + T + I + B \tag{1}$$

can be described by the sum of a geometric range ρ, the satellite and receiver clock offsets (δt,), as well as the tropospheric and ionospheric range delays (T, I) and an additive bias B. Considering two pseudorange observations obtained by tracking two distinct signals S_1 and S_2 of the same satellite at frequencies f_{S_1} and f_{S_2}, most of the above terms cancel when differencing both observations. The pseudorange difference

$$\begin{aligned} P_{S_1} - P_{S_2} &= (I_{S_1} - I_{S_2}) + (B_{S_1} - B_{S_2}) \\ &= 40.31\,\mathrm{m^3 s^2} \cdot \left(\frac{1}{f_{S_1}^2} - \frac{1}{f_{S_2}^2} \right) \cdot \mathrm{STEC} + \mathrm{DCB}_{S_1 - S_2} \,. \end{aligned} \tag{2}$$

can thus be expressed as the sum of the differential ionospheric path delay $I_{S_1} - I_{S_2}$ and a differential code bias

$$\mathrm{DCB}_{S_1 - S_2} = B_{S_1} - B_{S_2} \,. \tag{3}$$

Neglecting higher-order contributions the ionospheric path delays can further be related to the Slant Total Electron Content (STEC). Obviously, the pseudorange difference for noise- and multipath-free observations directly provides the corresponding DCB, if two signals (or signal components) on a common frequency are considered. Among others, this facilitates the determination of C/A-P(Y) and L2C-P(Y) biases on the GPS L1 and L2 frequency. The impact of STEC uncertainties is also notably suppressed for closely matching signal frequencies which benefits the determination of code biases among Galileo E5a, E5b, and E5ab observations.

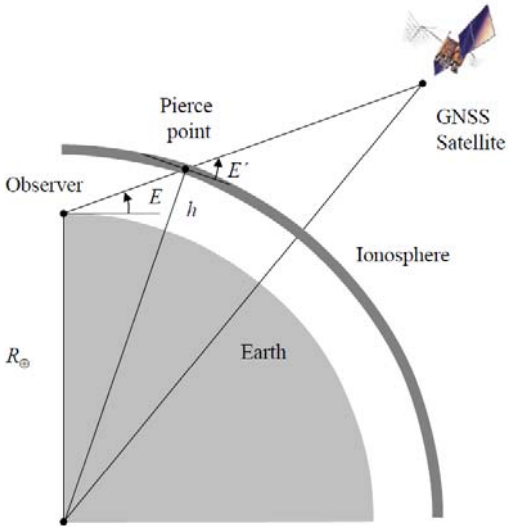

Figure 2 Single-layer ionosphere model

For further processing, the slant TEC is commonly described by the product

$$\mathrm{STEC} = \mathrm{VTEC} \cdot m(E) \tag{3}$$

of the vertical TEC (VTEC) and an elevation-dependent mapping function $m(E)$. In the most simple case of a single-layer model ([12], [9]), the ionosphere is considered as a thin shell of constant altitude h (Fig. 2). The mapping function

$$\mathrm{m}(E) = \frac{1}{\sin(E')} = \frac{1}{\sqrt{1 - \cos^2(E')}} \tag{4}$$

is then determined by the elevation E' at the ionospheric pierce point (IPP). From the Earth-observer-IPP triangle the pierce point elevation is obtained as

$$\cos(E') = \frac{R_\oplus}{R_\oplus + h} \cos(E) \,. \tag{5}$$

for a satellite observed at elevation E from the given site.

For estimation of the global VTEC distribution, dual-frequency GPS (or, more generally, GNSS) observations from a worldwide station network are jointly processed [9] and the geographic VTEC variation is described by a linear combination of spherical harmonics or other base-

functions or, alternatively, interpolation across a set of 2D or 3D grid points (see [12]-[14] and references therein). The coefficients of this parameterization can then be estimated along with satellite- and site-specific DCBs for the employed signal.

While the estimation of ionospheric parameters is commonly expected to benefit from better spatial and temporal resolution if multiple GNSS constellations and signals are processed, existing ionosphere and DCB estimation software is still largely focused on GPS(+GLONASS) processing. As such, only sparse information on differential code biases of new navigation satellite systems is available so far and mostly restricted to group delay parameters made available within the broadcast ephemeris messages. To fill this gap, an alternative and computationally less intensive approach has been pursued, which builds on the availability of global ionosphere maps to describe the contribution of ionospheric path delays in the difference of dual-frequency code observations.

In a first step, the combined satellite-plus-receiver DCBs are determined for all contributing sites and all observed satellites. Making use of (2)-(5), the combined satellite-plus-receiver DCB may be obtained from the arithmetic mean

$$\mathrm{DCB}_{\mathrm{S}_1-\mathrm{S}_2} = \frac{1}{n}\sum_{i=1}^{n}\left[\left(P_{\mathrm{S}_1} - P_{\mathrm{S}_2}\right) - \Delta I\right]_i \qquad (6)$$

of a suitably large set of ionosphere corrected pseudorange observations where the inter-frequency difference of the ionospheric path delay

$$\Delta I = 40.31\,\mathrm{m^3 s^2}\cdot\left(\frac{1}{f_{\mathrm{S}_1}^2} - \frac{1}{f_{\mathrm{S}_2}^2}\right)\cdot m(E)\cdot \mathrm{VTEC} \qquad (7)$$

is modeled by the known VTEC and a single-layer mapping function. As an underlying assumption, the DCB is considered to be constant over the period of the data arc. In addition receiver noise and multipath errors are assumed to have a zero mean average over the data arc. For practical reasons, a 1-day data arc is adopted, making use of daily RINEX observation files at a 30 s sampling rate. Furthermore, a minimum elevation limit of 20° is applied for observations considered in the DCB estimation. This value has been chosen to reduce the impact of ionosphere modeling errors at low elevations while maintaining coverage of geostationary satellites by an adequate number of widely distributed stations.

For the purpose of illustration, the difference of E5a and E1 pseudoranges is shown in Fig. 3. Following the model-based correction of the ionospheric path delays, a DCB of about -20 ns (-6 m) is obtained.

The above approach matches the single-station bias determination concept proposed in [15], except for the direct processing of unsmoothed code observations. Carrier phase smoothing of code observations or the use of code-leveled carrier phase observations results in a notably reduced noise level for the instantaneous ionospheric parameter estimation. However, it does not affect the estimated code bias obtained from a mean value over the entire data arc.

Following the estimation of satellite-plus-receiver-biases for all sites and satellites, individual satellite and receiver DCBs are obtained in a second step. Here, it is assumed that biases generated in the transmitter chain and the receiver are additive and fully independent of each other. Consequently, the overall DCB may be separated into the sum of a receiver-specific contribution and a satellite-specific part:

$$\mathrm{DCB} = \mathrm{DCB}^{\mathrm{sat}} + \mathrm{DCB}^{\mathrm{rcv}} \quad . \qquad (8)$$

While this is not true in general (see, e.g. [16]-[18]) due to the multiplicative nature of the transfer function of the entire signal chain, it represents a standard approximation in GNSS bias analysis and is likewise applied in the present work.

Denoting by

$$\boldsymbol{x}^{\mathrm{sat}} = (\mathrm{DCB}^{\mathrm{sat},1},\ldots,\mathrm{DCB}^{\mathrm{sat},n})^T \quad . \qquad (9)$$

and

$$\boldsymbol{x}^{\mathrm{rcv}} = (\mathrm{DCB}^{\mathrm{rcv},1},\ldots,\mathrm{DCB}^{\mathrm{rcv},m})^T \quad . \qquad (10)$$

the vectors of DCBs for n satellites and m stations and

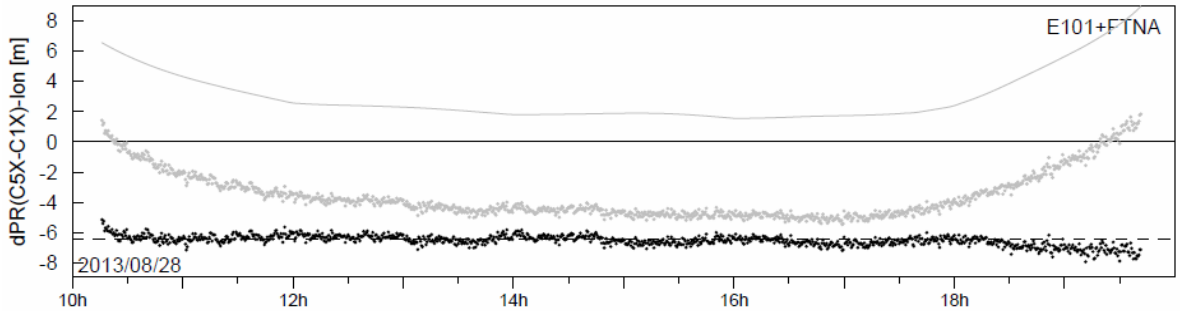

Figure 3 Difference of E5a and E1 pseudoranges of Galileo PRN IOV-1 satellite (SVN101) tracked from the FTNA station before (shaded) and after (black) ionospheric correction. The modeled ionospheric path delay difference based on CODE global ionosphere maps is indicated by a shaded line. The dashed line indicates the estimated satellite-plus-receiver DCB.

by

$$\boldsymbol{z} = (\mathrm{DCB}^1, \ldots, \mathrm{DCB}^k)^T \quad . \tag{10}$$

the vector of k "observed" satellite-plus-receiver DCBs as derived from (6), the unknown biases may be obtained by minimizing the loss function

$$J = \left\| \boldsymbol{z} - \boldsymbol{A}\boldsymbol{x}^{\mathrm{sat}} - \boldsymbol{B}\boldsymbol{x}^{\mathrm{rcv}} \right\|^2 \quad . \tag{11}$$

Based on the additive DCB model (8) , the partial derivatives

$$A_{ij} = \partial z_i / \partial x_j^{\mathrm{sat}} \quad \text{and} \quad B_{ij} = \partial z_i / \partial x_j^{\mathrm{rcv}} \quad . \tag{12}$$

are equal to one for just a single element in each row of $\boldsymbol{A}$ and $\boldsymbol{B}$ but zero otherwise. The resulting normal equations matrix $(\boldsymbol{A}, \boldsymbol{B})^T (\boldsymbol{A}, \boldsymbol{B})$ exhibits a rank deficiency since a bias common to all satellites cannot be distinguished from a corresponding bias common to all receivers. The rank deficiency may be removed by fixing a single receiver bias or by imposing a zero-mean condition for the satellites. While the former approach is suitable for use with calibrated reference receivers in a GNSS control segment, the latter is commonly applied within the IGS and likewise adopted in this study. Furthermore, the loss function (11) is modified by a weighting matrix, which reflects the standard deviation of the ionosphere- corrected pseudorange differences $\left(P_{S_1} - P_{S_2}\right) - \Delta I$ in (6). In this way the varying quality of the satellite-plus-receiver DCBs can be taken account, which is caused by pseudorange measurement errors and the varying performance of the single-layer ionosphere model.

PERFORMANCE ASSESSEMENT

The DCB estimation scheme presented above differs in various aspects from more elaborate techniques which jointly estimate ionospheric and bias parameters in a common adjustment process. Aside from the inevitable impact of measurement errors, it relies on the quality of the global ionosphere maps employed from the slant TEC correction. Prior to presenting and discussing more detailed results, an effort shall therefore be made to assess the overall performance of the method. The following performance indicators are employed for this purpose:

- Consistency of estimated GPS satellite DCBs with monthly values derived by the CODE analysis center of the IGS
- Day-to-day variations of estimated satellite and receiver biases for selected signals

For a first assessment, the DCBs for GPS P(Y)-code tracking on L1 and L2 are compared in Figure 4. Aside from a mean offset of -0.05 ns, the biases of individual GPS satellites exhibit a standard deviation of 0.20 ns across the entire constellation when compared to the CODE reference solution. Daily biases for a given satellite exhibit a scatter of about 0.06-0.08 ns (1σ) across the monthly average.

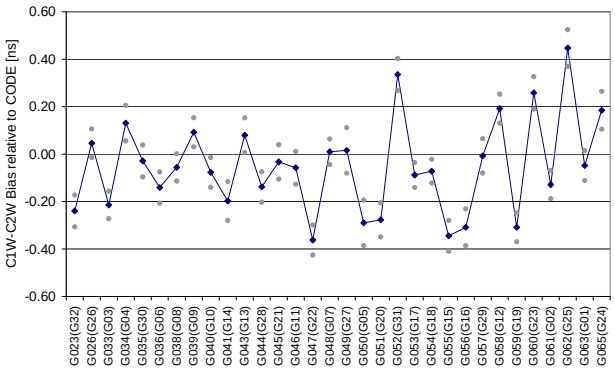

Figure 4 Difference of GPS C1W-C2W (=P1-P2) DCBs determined in this study as compared to the monthly DCB product of CODE for the month of January 2013. The mean offset of the daily DCB solutions from the CODE reference is shown in blue. 1σ bounds of the daily solutions relative to the mean values are indicated by grey markers.

A similar comparison is provided in Fig. 5 for the inter-signal bias of L1 P(Y) and L1 C/A tracking. Due to the common frequency, errors in the ionospheric modeling do not affect the estimated DCBs and the day-to-day variation is in fact substantially decreased to a representative value of about 0.01 ns (1σ). Nevertheless, obvious differences between DCBs estimated in this study and the CODE values used as reference may be noted. These differences exhibit a standard deviation of about 0.3 ns across the entire constellation, which even exceeds that of the C1W-C2W inter-frequency bias. It may be concluded that the observed scatter is largely driven by differences in the employed network and receiver types.

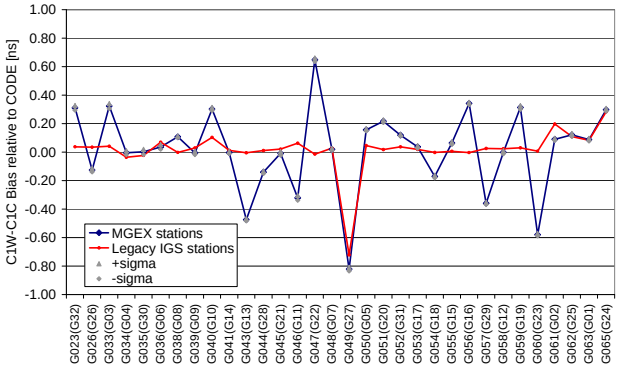

Figure 5 Difference of GPS C1W-C1C (=P1-C1) DCBs determined in this study as compared to the monthly DCB product of CODE for the month of January 2013 (blue: DCBs based on MGEX stations; red: DCBs based on legacy IGS stations).

To substantiate this interpretation, a complementary C1W-C2W DCB solution has been obtained from a much larger set of legacy IGS stations closely matching those used in the CODE analysis. While at most 41 (of 85) MGEX stations contribute both C1W and C1C observations an almost 3-times larger number of contributing stations (114 out of 222) was available in the IGS net-

work. As can be seen from Fig. 5, a much better agreement with CODE results is obtained in this case with the exception of SVN49. The latter spacecraft exhibits a large satellite-internal multipath (see [19]-[20]) and the resulting inter-signal code biases vary largely with the employed receiver technology.

Overall, the above comparison suggests that DCBs can be determined with a representative accuracy of a few tenths of nanoseconds with the proposed approach, if a sufficiently large number of stations (typically >30) contributes the observations types of interest.

RESULTS AND DISCUSSION

Within this section, results for the satellite biases of modernized GPS signals as well as Galileo and BeiDou are presented and discussed. Furthermore, key characteristics of station biases are presented and the dependence on receiver types is highlighted.

Modernized GPS

Up to fall 2013, the modernized civil L2 signal (L2C) has been transmitted by a total of 8 Block IIR-M satellites (including the unhealthy SVN49 s/c) as well as four satellites of the latest Block IIF generation. Since geodetic GNSS receivers traditionally support a semi-codeless tracking of the L2 P(Y) signal on the same frequency, this signal provides a natural reference for the estimation of L2C-related differential code biases. In accord with the three tracking modes employed by receivers of the MGEX network (see Table 1), distinct C2W-C2S, C2W-C2W and C2W-C2X biases have been determined. All of these exhibit a very small day-to-day variation (typically less than 0.04 ns) and peak values of about ±1 ns with respect to the constellation mean (Fig. 6).

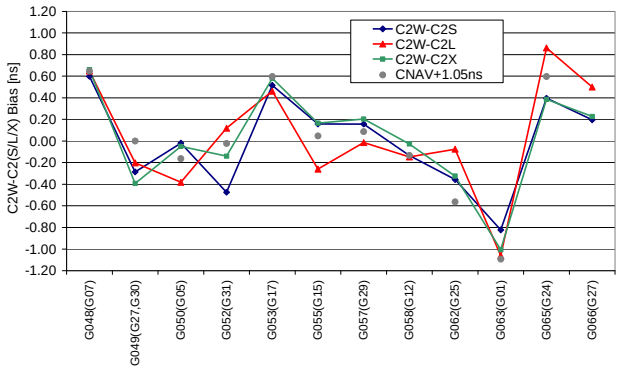

Figure 6 Differential code biases between P(Y) and L2C tracking on L2 (mean values April-June 2013). For comparison, differential code biases between P(Y) and L2C based group delay corrections transmitted during the CNAV test campaign in June 2013 are indicated by grey circles.

Differences of DCBs for the individual L2C tracking modes exhibit a standard deviation of about 0.3 ns across the constellation, which is significant compared to the overall size of the DCBs but still at the uncertainty level of the DCB estimation discussed in the previous section. Unfortunately, the lacking distinction of L2C tracking modes within the old RINEX2 format inhibits use of a larger set of tracking stations from the legacy IGS network for a more detailed investigation of this aspect. It appears advisable, though, to carefully distinguish the three L2C tracking modes if DCB accuracies well below a carrier phase wavelength (20 cm or 0.7 ns) are desired.

As part of the new L2 and L5 CNAV navigation message, inter-signal corrections will be transmitted, which reflect the DCBs of these signals relative to the L1 P1 signal (see [21],[7],[5]). A first CNAV test transmission was performed in June 2013 [22] during which ISC_{L2C} values (corresponding to C1W-C2S/L/X DCBs) were transmitted for all L2C-capable satellites except SVN49 and the most recently launched IIF-4 satellite (SVN66, PRN27). A comparison of broadcast ISCs with values derived in this study is shown in Fig. 7.

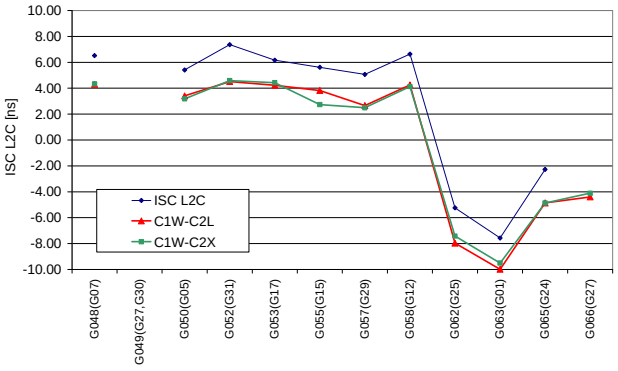

Figure 7 Differential code biases between L1 P(Y) and L2C as compared to broadcast ISC_{L2C} parameters from the CNAV tracking campaign.

Aside from a mean offset of 2.3 ns, the difference between broadcast ISCs and DCBs derived from ionosphere-corrected pseudorange observations exhibits a scatter of 0.3-0.4 ns. This is compatible with uncertainty estimates for other DCB types given above, if one takes into account that only few stations (11 for DCB(C1W-C2L) and 30 for DCB(C1W-C2X)) allow a joint tracking of the respective signals for the bias estimation.

A more favorable agreement at the 0.1-0.2 ns level is achieved when computing the differential code bias

$$\mathrm{DCB(C2W-C2)} = \frac{f_1^2 - f_2^2}{f_2^2} \cdot \mathrm{TGD} + \mathrm{ISC_{L2C}} \qquad (13)$$

between P(Y) and L2C from the combination of TGD and ISC_{L2C} parameters (cf. [23]). The respective values are shown in Fig. 6, where a bias of 1.05 ns has been added to achieve a zero-mean constellation average. The best overall agreement is achieved in comparison with C2W-C2X DCBs derived in the present study, which may indicate that the broadcast parameters are obtained from a corre-

sponding set of receivers. However, the actual source of the transmitted ISCs has not been reported, and information on the expected accuracy is not presently available.

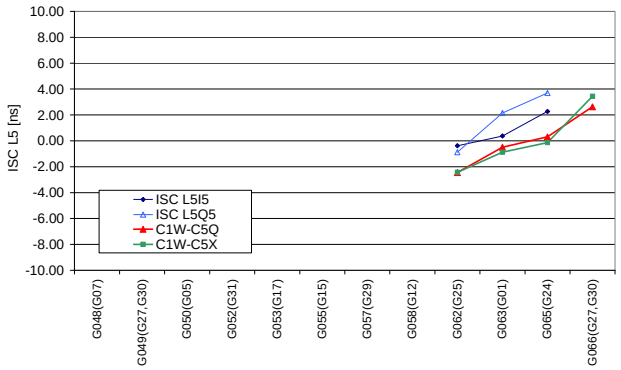

Figure 8 Differential code biases between L1 P(Y) and L5 as compared to broadcast $ISC_{L5I5/L5Q5}$ parameters from the CNAV tracking campaign.

A comparison of broadcast ISCs for the L5 signal with values from the present study is, furthermore, provided in Fig. 8. The two ISC values for the data signal (ISC_{L5I5} and the pilot signal (ISC_{L5Q5}) transmitted in the CNAV test show a mean offset of about 2 ns from the present analysis, but agree less well among each other than the DCB(C1W-C5Q) and DCB(C1W-C5X) code biases. Again, however, the origin of the broadcast ISC parameters is unknown, which inhibits further interpretation of the these observations.

BeiDou

The current BeiDou constealltion transmits signals on a total of three frequencies: B1 (E2, near L1), B2 (E5b), and B3 (near E6). In-phase components of the B1 and B2 are considered as Open Service signals, while the remaining four signals (B3 in-phase and B1/B2/B3 quadrature components) are commonly expected to be restricted signals of an Authorized Service. Nevertheless, tracking of the B3-I component is presently supported by various receivers in the MGEX network due to the known structure of the employed ranging codes.

Differential code biases derived from MGEX observations of BeiDou are shown in Fig. 9. The results cover the operational satellites (SVN C003-C016, PRN 01-14) as well as the first test satellite (SVN C001, PRN C30) and have been normalized by a zero-mean constraint across the full set of 15 spacecraft. With the exception of the first two space vehicles (C30, C01), the resulting DCBs biases are confined to a range of ±10 ns, which is similar to the range of L1/L2 code biases encountered in GPS. On the other hand, the day-to-day variations of the estimated biases exhibit a representative standard deviation 0.2 ns (and peak values of 0.5 ns), which is notably larger than for GPS. This can, in part be attributed to the limited number of stations in the Asia-Pacifica region observing the GEO and IGSO satellites as well as the lacking global coverage for MEO satellites. Other aspects that might affect the DCB calibration performance include long-periodic multipath errors in the tracking of geostationary BeiDou satellites (caused by a quasi-static viewing geometry) as well as code-carrier inconsistencies [24]-[25] that suggest the presence of satellite-induced group delay variations across the antenna.

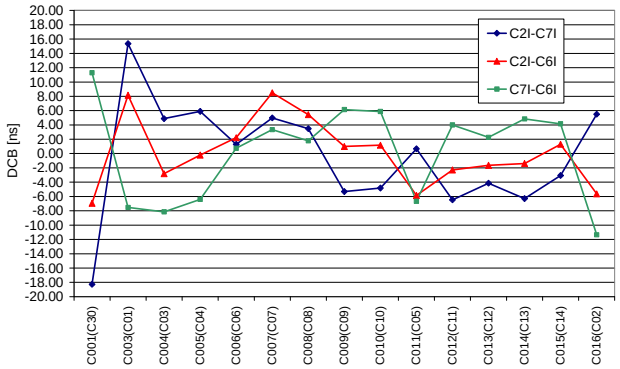

Figure 9 Differential code biases of BeiDou signals as derived from GIM-corrected B1, B2 and B3 pseudorange observations (mean values for Jan. 2013).

While GPS, GLONASS, Galileo, QZSS and IRNSS refer their broadcast clock offsets to a ionosphere-free combination of dual-frequency pseudoranges [23], BeiDou has adopted the B3 signal as the primary clock reference [26]-[27]. For use with other signals or signal combinations, tow timing group delay parameters (TGD1, TGD2) are provided in the BeiDou navigation message, that describe corrections for use with B1 and B2 signals, respectively, and can thus be interpreted as B1-B3 and B2-B3 differential code biases. Even though the current B1 Open Service Signal ICD of BeiDou specifies only the TGD1 parameter, the presence of TGD2 can be inferred from inspection of the raw navigation data frames [27] and both parameters are now routinely collected within the MGEX project.

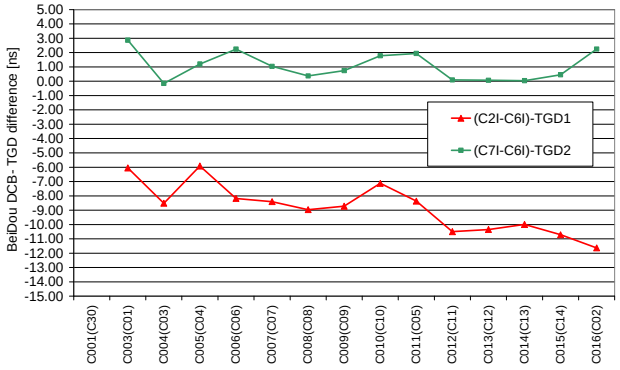

Figure 10 Difference between BeiDou DCBs estimated in this study and corresponding timing group delay parameters from the BeiDou navigation message.

As can be recognized from Fig. 10, the TGD values are not normalized to a constellation mean of zero and exhibit a notable mean offset from the DCBs determined here.

Even worse, a pronounced scatter (±1.5 ns for TGD1, ±3 ns for TGD2) can be noted, which by far exceeds the expected uncertainty of the present DCB estimates. The cause of this discrepancy is not known at present, but may be related to differences between the B3-I and B3-Q signal component or the incorporation of antenna offsets into the published TGD values. Further analysis will be required to better understand this finding and to assess the performance of the various group delay parameters in multi-frequency positioning solutions. It is evident though, that an independent DCB monitoring for all "public" signals is vital for an optimum understanding and utilization of the BeiDou navigation system.

Galileo

Aside from the E1 Open Service, Galileo offers a total of three signals (E5a, E5b and E5AltBOC) in the combined E5ab band that can be accessed by civil receivers. For all of these signals both data- and pilot-codes are transmitted concurrently. Observations may thus be based on tracking of an individual pilot or data channel or a combination thereof. As summarized in Table 2, current receivers utilize either a pure pilot-tracking mode (indicated by C1C and C5Q/C7Q/C8Q observation types) or a combined mode (indicated by C1X and C5X/C7X/C8X observation types) for Galileo. Due to the lack of receivers supporting concurrent tracking in multiple modes, it is not possible to directly observe differential code biases between pilot and data components of the various signals. Instead, distinct inter-frequency DCBs are derived within this study for the two tracking modes (pilot or combined). In all cases the DCBs are formed with respect to the E1 signal, which serves as a common reference.

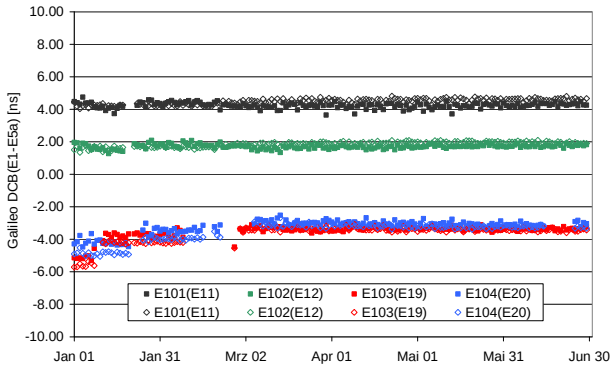

Figure 11 Galileo E1-E5a differential code biases. Pilot-only DCBs (E1C-E5Q) are indicated by solid squares, the corresponding biases for combined pilot-data tracking are marked with open diamonds.

Time series of daily E1-E5a differential code biases for the four Galileo In-Orbit-Validation (IOV) satellites are shown in Fig. 11. During the first quarter of the year various jumps in the DCBs of the most recently launched satellites (IOV-3/PRN E19 and IOV-4/PRN E20) may be noted, which coincide with data gaps and can potentially be attributed to equipment or configuration changes in the signal generation chain. Within the second quarter of the year a high stability of the observed biases can be noted. Here, day-to-day-variations and possible residuals drifts result in a standard deviation of about 0.1 ns.

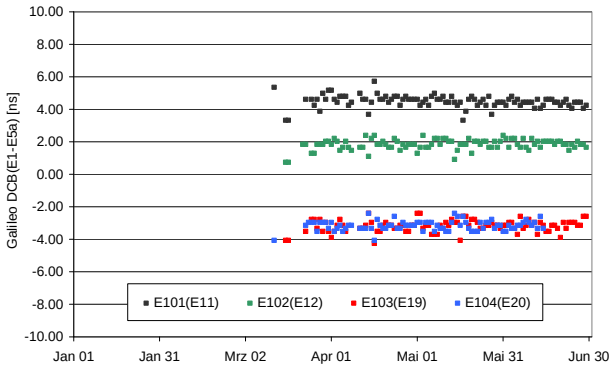

Figure 12 Galileo E1-E5a differential code biases from BGD_{E5aE1} Broadcast Group Delay parameters transmitted in the Galileo navigation message.

For comparison, Fig. 12 shows the corresponding differential code bias

$$DCB(E1-E5a) = -\frac{f_{E1}^2 - f_{E5}^2}{f_{E1}^2} \cdot BGD_{E1E5a} \qquad (14)$$

as obtained from BGD_{E5aE1} broadcast group delay parameters transmitted in the Galileo I/NAV navigation message since March of this year. Evidently, a zero-average constraint is applied in the operational ionosphere and bias estimation process similar to the present study. As a result, a good agreement of the mean bias values for the individual satellite can be noted from the direct comparison of Figs. 11 and 12. However, a much larger scatter of the broadcast values (roughly 0.3 ns standard deviation) is obvious, which reflects the notably smaller network of presently 12 Galileo sensor stations [28].

Table 2 Mean values of Galileo IOV DCBs for April-June 2013

DCB	E101 (E11) [ns]	E102 (E12) [ns]	E103 (E19) [ns]	E104 (E20) [ns]
C1C-C5Q	4.25	1.75	-3.31	-3.03
C1X-C5X	4.51	1.87	-3.48	-3.27
C1C-C7Q	4.59	1.43	-3.50	-2.85
C1X-C7X	4.89	1.45	-3.74	-2.92
C1C-C8Q	4.39	1.48	-3.19	-3.01
C1X-C8X	4.53	1.51	-3.28	-3.10

Mean values of the differential code biases for E5a, E5b and E5ab signals relative to E1 over a 3 months period are summarized in Table 2. Differences of DCBs for pilot-only tracking vs. combined tracking range from 0.1-0.3 ns, which is slightly larger than the scatter of the daily DCB estimates but may well reflect the impact of different sets of tracking stations used to determine the two types of biases.

Furthermore, a close match of biases for the individual and combined E5a/E5b frequency bands may be noted. Differences between E5a-E1, E5b-E1 and E5ab-E1 DCBs for all IOV satellites amount to less than 0.5 ns, which reflects a high quality of the signal generation and transmission chain despite the extreme bandwidth of the combined E5ab band.

As a final note, it is emphasized that no observations of the first two Galileo test satellites, GIOVE-A and –B, were considered in this study. Compared to the IOV satellites, these spacecraft exhibit widely different E5a/b/ab-E1 biases that were inconsistently handled by individual receiver manufacturers. However, both satellites were deactivated long before the start of the present analysis period.

Station Biases

Based on the assumed separability of differential code biases into a GNSS satellite contribution and a receiver(+antenna) contribution, site specific DCBs have been obtained as part of the MGEX data processing for the supported constellations and signals. Other than the satellite-specific DCBs, which need to be explicitly considered in the measurement model, the receiver DCBs are usually lumped with other parameters (such as the receiver clock offset, system time offsets, inter-system biases) when performing a point positioning [23]. However, pronounced differences between the DCBs of different receiver families may typically be observed, which affects the alignment of time scales and inter-frequency biases in a multi-GNSS processing. Also, proper knowledge of receiver-receiver DCB differences is of interest in mixed-receiver multi-GNSS relative navigation problems to speed up the ambiguity resolution process [29].

Since a detailed presentation of receiver+antenna biases for all MGEX stations and available signals is well beyond the scope of the current paper, we confine ourselves to a discussion of key characteristics of individual receiver types. As shown in Table 3, site-specific DCBs for signals on different frequencies cover a typical range of 10-15 ns when considering receivers of a given family, while DCBs for signals of common frequency (such as GPS L1 C/A and P(Y)) exhibit a much smaller scatter at the 1 ns level across similar receivers.

In both cases these budgets comprise the combined effects of receiver and antenna biases. A comparison of station biases for groups of similar receivers but different antennas suggests antenna-related bias differences at the 5 ns level for some of the observed signals. As an extreme case, the USN4 station of the United States' Naval Observatory shows a 15 ns difference of the E1-E5a bias compared to other sites with the same receiver type (Septentrio PolaRx4). This can essentially be attributed to the use of a legacy L1/L2 AOAD/M_T antenna that has not been designed for L5 reception. The atypical antenna bias also affects the collocated USN5 station which constitutes the only NovAtel OEM6 receiver in the MGEX network. Accordingly, the corresponding biases in Table 3 should not be considered as representative for this receiver family. Further investigations and tests with collocated receivers will be required to properly isolate the impact of the antenna- and receiver-specific contributions of the station biases.

Comparing the inter-frequency biases of different receiver families, systematic offsets of 20-40 ns can be observed for GPS (e.g. C1C-C2W DCB difference Leica-Trimble). Even larger differences may be encountered with some of the new constellations as evidenced by the C1C-C7Q DCB difference of Leica and Septentrio receivers). As an extreme case, DCB differences of up to 100 ns can bee observed for the Javad Delta-G3TH (rev. 8) receiver with Galileo E5b and BeiDou B2 tracking support in comparison to other receiver types.

Table 3 Representative range of receiver DCBs for different signals and receiver brands as listed in Table 1. Signals are indicated by their RINEX signal designators. Values in brackets are derived from a single receiver in the MGEX network and require further consolidation.

Constellation	Signals	Javad	Leica	NovAtel	Septentrio	Trimble
GPS	C1C-C2W	+5…+15 ns	+15…+25 ns	(+10 ns)	+5…+10 ns	-20…-5 ns
	C1C-C5Q		+10…+15 ns	(-12 ns)	-5…+0 ns	
	C1C-C5X	-15…-5 ns				-25…-10 ns
	C1W-C1C	-2.5…-1.5 ns			-2.0…-1.5 ns	
	C1W-C2W	-5…+15 ns			+5…+10 ns	
	C2W-C2S		-2.6…-2.2 ns			
	C2W-C2L				-1.0…-0.5 ns	
	C2W-C2X	-2.0…-0.5 ns				-0.5…+1.5 ns
Galileo	C1C-C5Q		+5...+15 ns	(-15 ns)	-5...+0 ns	
	C1X-C5X	-10...+0 ns				-10...+5 ns
	C1C-C7Q		-55...-45 ns		+5...+15 ns	
	C1X-C7X	(+105 ns)				+0...+10 ns
	C1C-C8Q		-60...-50 ns		+5...+10 ns	
	C1X-C8X	(+15 ns)				-5...+5 ns
BeiDou	C2I-C7I	(+115 ns)			+10...+20 ns	+20...+30 ns
	C2I-C6I					+40...+55 ns
	C7I-C6I					+20...+30 ns

Overall, the values summarized in Table 3 may serve for a better understanding of receiver-related biases in multi-GNSS clock offset solutions for GNSS satellites as well as differential receiver biases in terrestrial networks.

SUMMARY AND CONCLUSIONS

Differential code biases are well known to affect the precise processing of GNSS observations and are continuously monitored for the legacy GPS and GLONASS signals. With the advent of new GNSS constellations and modernized signals, users are confronted with an ever increasing plethora of signals, tracking modes and associated biases. To cope with this problem, a DCB estimation process has been implemented, which determines inter-signal and inter-frequency code biases from the mean difference of commonly-tracked pseudorange observations after correction of the relative ionospheric path delay with a global ionosphere map. While potentially less accurate than a joint estimation of ionospheric and bias estimation, the approach facilitates and efficient processing of large data sets and has been used to determine DCBs for modernized GPS signals as well as the Galileo and BeiDou system using observations from the MGEX network of the IGS.
Depending on the number of stations jointly tracking a given constellation and signal set, a day-to-day repeatability at the 0.05-0.3 ns level has been obtained for the estimated satellite biases. Station-specific DCB often exhibit larger variations at the 1 ns level, which may be attributed to imperfections of the ionospheric correction. However, further investigations will be required to assess the actually stability of station biases and the potential benefit of refined, local estimates of ionospheric path delays on the bias estimation.

A good agreement (<0.2ns) of DCBs derived in this study with broadcast group delay parameters was obtained for GPS L2C (w.r.t. to L2 P(Y)) as well as Galileo E5a/b (relative to E1). On the other hand, differences of a few ns were identified for signals of the Chinese BeiDou system, which require further attention. Among others, it is not presently clear to what extent the (partly unofficial) BeiDou TGD parameters include additional contributions such as antenna offsets that would inhibit a direct comparison with pure DCB values as derived in this study.

Concerning new navigation signals with distinct pilot and data components it could not be finally clarified whether (or to what extent) the biases depend on the selected signal component and tracking mode. For GPS L2C, differences exceeding the day-to-day stability of the DCB estimates were observed between tracking of the medium, long or combined code components, but those differences may well reflect the impact of the different sets of stations supporting a given tracking mode. For Galileo, satellite DCB differences derived from receivers with pilot-only tracking vs. combined pilot+data tracking are less than 0.5 ns (typically 0.3 ns), which makes it likewise difficult to distinguish network-related effects from true, signal-related bias differences.

Station DCBs (comprising receiver and antenna contributions) for some signals of the new constellations were found to show much higher systematic differences between receiver brands than known from GPS and the legacy L1/L2 signals. While this does not in any way affect the suitability of specific receiver types for multi-GNSS processing, it will require due attention in various applications. In particular, it will affect the estimation of satellite clock biases in a joint multi-GNSS orbit and clock determination process and thus the time scales realized in future IGS multi-GNSS ephemeris products. Likewise, multi-GNSS ambiguity resolution in heterogeneous receiver networks may be affected when neglecting the actual DCB differences.

REFERENCES

[1] Montenbruck O., Rizos Ch., Weber R., Weber G., Neilan R., Hugentobler U. (2013) “Getting a Grip on Multi-GNSS: The International GNSS Service MGEX Campaign”; GPS World 24(7), 44-49

[2] IGS (2013a) Homepage of the IGS Multi-GNSS Experiment. URL http://igs.org/mgex (alternate URL for access from China: http://igsws.unavco.org/mgex/)

[3] IGS (2013b) “RINEX – The Receiver Independent Exchange Format”; Version 3.02; IGS RINEX WG and RTCM-SC104, 3 April 2013.

[4] Falcone M., Binda S., Breeuwer E., Hahn J, Spinelli E., Gonzalez F., López Risueño G., Giordano P., Swinden R., Galluzzo G., Hedquist A. (2013) “Galileo on Its Own – First Position Fix”; Inside GNSS March-April 2013, 50-71.

[5] IS-GPS-705 (2011) “Navstar GPS Space Segment / User Segment L5 Interfaces”, Interface Specification IS-GPS-705, Revision B, 21 Sep. 2011, Global Positioning Systems Directorate.

[6] IS-GPS-800 (2010) “Navstar GPS Space Segment / User Segment L1C Interface”, Interface Specification IS-GPS-800, Revision A, 8 June 2010, GPS Wing, Los Angeles, CA.

[7] IS-GPS-200 (2012) “Navstar GPS Space Segment / Navigation User Segment Interfaces”; Interface Specification IS-GPS-200, Revision G, 5 Sep. 2012, Global Positioning Systems Directorate.

[8] Yinger C.H., Feess W.A., Di Esposti R., Chasko A., Cosentino B., Wilson B., Wheaton B. (1999) “GPS Satellite Interfrequency Biases”, ION GPS 1999, Cambridge, MA, June 1999, pp. 347-354.

[9] Hernández-Pajares M., Juan J.M., Sanz J., Orus R.,·Garcia-Rigo A., Feltens J.,·Komjathy A., Schaer S.C., Krankowski A. (2009) “The IGS VTEC maps: a reliable source of ionospheric information since 1998”, Journal of Geodesy 83:263–275. DOI 10.1007/s00190-008-0266-1

[10] Heise S., Jakowski N., Cooke D. (2005) “Ionosphere/plasmasphere imaging based on GPS navigation

measurements from CHAMP and SAC-C", In: Earth Observation with CHAMP. Springer Berlin Heidelberg, 471-476.

[11] Schaer S, Gurtner W, Feltens J (1998) "IONEX: The IONosphere map Exchange Format Version 1". Proceedings of the IGS AC Workshop, Darmstadt, Germany, 9-11 February 1998

[12] Schaer S (1999) "Mapping and predicting the Earth's ionosphere using the Global Positioning System". Geodaetisch-geophysikalische Arbeiten in der Schweiz, 59.

[13] Mannucci A.J., Wilson B.D., Yuan D.N., Ho C.H., Lindqwister U.J., Runge T.F. (1998) "A global mapping technique for GPS-derived ionospheric total electron content measurements". Radio Science 33:565–582.

[14] Li Z., Yuan Y., Li H., Ou J., Huo X. (2012) "Two-step method for the determination of the differential code biases of COMPASS satellites". Journal of Geodesy, 86(11), 1059-1076.

[15] Arikan F, Nayir H, Sezen U, Arikan O (2008) "Estimation of single station interfrequency receiver bias using GPS-TEC", Radio Science 43:RS4004. DOI: 10.1029/2007RS003785

[16] Phelts RE, Gao GX, Wong G, Heng L, Walter T,Enge P, Erker S, Thoelert S, Meurer M (2010) "Aviation Grade: New GPS Signals – Chips Off the Block IIF"; Inside GNSS July-Aug. 2010, 36-45

[17] Hauschild A (2012) "SVN 47 (PRN 22) Signal Anomaly". IGS Workshop on GNSS Biases, Jan. 18-19, 2012, Bern, Switzerland.

[18] Lestarquit L., Gregoire Y., Thevenon, P. (2012) "Characterizing the GNSS Correlation Function using a High Gain Antenna and Long Coherent Integration - Application to Signal Quality Monitoring"; IEEE/ION PLANS 2012, Myrtle Beach, South Carolina , April 2012, pp. 877-885.

[19] Hauschild A., Montenbruck O., Thoelert S., Erker S., Meurer M., Ashjaee J. (2012) "A Multi-Technique Approach for Characterizing the SVN49 Signal Anomaly - Part 1: Receiver Tracking and IQ Constellation"; GPS Solutions 16(1):19-28 DOI 10.1007/s10291-011-0203-2

[20] Thoelert S., Meurer M., Erker S., Montenbruck O., Hauschild A., Fenton P. (2012) "A Multi-Technique Approach for Characterizing the SVN49 Signal Anomaly - Part 2: Chip Shape Analysis"; GPS Solutions 16(1):29-39. DOI 10.1007/s10291-011-0204-1

[21] Tetewsky A, Ross J, Soltz A, Vaughn N, Anzperger J, O'Brien Ch, Graham D, Craig D, Lozow J (2009) "Making Sense of Inter-Signal Corrections – Accounting for GPS Satellite Calibration Parameters in Legacy and Modernized Ionosphere Correction Algorithms", InsideGNSS, July-Aug. 2009, 37 -48a.

[22] Montenbruck, O., Langley, R.B., Steigenberger, P. (2013) "First Live Broadcast of GPS CNAV Messages"; GPS World, Vol. 24, No. 8, August 2013, pp. 14-15; URL http://www.gpsworld.com/2c-or-not-2c-the-first-live-broadcast-of-gps-cnav-messages/

[23] Montenbruck O., Hauschild A. (2013) "Code Biases in Multi-GNSS Point Positioning"; ION International Technical Meeting 2013, 28-30 Jan. 2013, San Diego.

[24] Montenbruck O, Hauschild A, Steigenberger P, Hugentobler U, Riley S (2012) "A COMPASS for Asia: First Experience with the BeiDou-2 Regional Navigation System", IGS Workshop 2012, 23-27 July 2012, Olsztyn, Poland.

[25] Perello Gisbert J.V., Batzilis N., Lopez Risueño G., Alegre Rubio J. (2012) "GNSS Payload and Signal Characterization using a 3m Dish Antenna", ION GNSS 2012, Nashville, TN, September 2012, pp. 347-356.

[26] Wu X, Hu X, Wang G, Zhong H, Tang C (2013) "Evaluation of COMPASS ionospheric model in GNSS positioning", Advances in Space Research 51:959–968. DOI 10.1016/j.asr.2012.09.039

[27] Montenbruck, O., Steigenberger, P. (2013) "The BeiDou Navigation Message", IGNSS Symposium 2013, 16-18 July 2013, Gold Coast, Qld, Australia

[28] Lucas Rodriguez R. (2013) "Galileo IOV Status and Results"; ION-GNSS-2013, 20 Sep. 2013, Nashville, TN.

[29] Odijk D., Teunissen P. (2013) "Estimation of Differential Inter-System Biases Between the Overlapping Frequencies of GPS, Galileo, BeiDou and QZSS"; 4th International Colloquium Scientific and Fundamental Aspects of the Galileo Programme, 4-6 Dec. 2013, Prague, Czech Republic.